Roles of Histidine 31 and Tryptophan 34 in the Structure, Self-Association, and Folding of Murine Interleukin-6†

Jacqueline M. Matthews,‡ Larry D. Ward,‡,§ Annet Hammacher,‡ Raymond S. Norton,|| and Richard J. Simpson*,‡

Joint Protein Structure Laboratory, Ludwig Institute for Cancer Research, and the Walter and Eliza Hall Institute of Medical Research, Parkville, Victoria 3050, Australia, and Biomolecular Research Institute, Parkville, Victoria 3052, Australia

Received December 2, 1996; Revised Manuscript Received February 10, 1997⊗

ABSTRACT: Interleukin-6 (IL-6) is a multifunctional cytokine which is involved in a broad spectrum of activities such as immune defense, hematopoiesis, and the acute phase response, as well as in the pathogenesis of multiple myeloma. A series of murine IL-6 (mIL-6) mutants, H31A, W34A, and H31A/W34A, were constructed to investigate the roles of His31 and Trp34 in the structure, conformational stability, time-dependent aggregation, folding, and spectral properties of mIL-6. The characteristic pH-dependent quenching of fluorescence of mIL-6 at low pH was shown to be caused by an interaction between Trp34 and protonated His31 at low pH and not associated with Trp157. Denaturant-induced equilibrium unfolding experiments monitored by fluorescence and far-UV CD showed that the increased quantum yield and blue shift of the wavelength of the emission maximum observed for mIL-6 at moderate denaturant concentrations were also associated with Trp34, rather than Trp157. The tendency to form aggregation-prone unfolding intermediates, as judged by poor fits to a two-state unfolding mechanism, low *m* values (slopes of the unfolding curve in the transition region), and the range of denaturant concentrations over which these intermediates formed, was shown to be higher for H31A than mIL-6 but significantly lower for W34A and H31A/W34A. These differences were most pronounced at pH 7.4 and correlated with the tendencies of the proteins to aggregate at high protein concentrations in the absence of denaturant. As judged by the ^{1}H NMR chemical shifts of the aromatic residues, the global conformations of H31A and W34A were not significantly different from that of mIL-6. Nuclear Overhauser effects (NOE) between the side chains of His31 and Trp34 were consistent with the indole side chain of Trp34 being oriented toward the face of the imidazolium side chain of His31, an arrangement consistent with our estimates of a low interaction energy (0.4−0.6 kcal/mol) between these side chains. A shift in the pK_a of the His31 side chain in W34A (+0.3 unit) suggested that, in the absence of Trp34, His31 could interact with other residues. Further mutations in this region should yield forms of mIL-6, even less prone to aggregation, which would be more suitable for NMR studies. Mutation of His31 and Trp34 to alanine did not significantly alter the mitogenic activity of the mutants on mouse hybridoma 7TD1 cells, even though the corresponding region of human IL-6 has been shown to be important for biological activity.

Interleukin-6 (IL-6)[1] is a multifunctional cytokine which plays a central role in hematopoiesis and a variety of host defense mechanisms, including immune responses and acute-phase reactions (Akira et al., 1993; Narazaki & Kishimoto, 1994). Overexpression of IL-6 has been implicated in a number of disease states, such as multiple myeloma (Klein et al., 1995), rheumatoid arthritis, Castleman's disease, AIDS, psoriasis, Kaposi's sarcoma, sepsis, and osteoporosis (Hirano, 1994). The association of IL-6 with clinical disorders has prompted intense interest in the development of small molecule inhibitors of IL-6 action as potential therapeutic agents in the treatment of IL-6 associated diseases. A thorough understanding of the structure−function relationships of IL-6, including a high-resolution structure of the protein, is a prerequisite for the rational design of small molecule IL-6 antagonists.

While no structure of IL-6 has yet been published,[2] several groups have used the structures of human and bovine granulocyte colony stimulating factor (Hill et al., 1993; Lovejoy et al., 1993), a closely related cytokine, to construct homology models of IL-6 (Ehlers et al., 1994; Hammacher et al., 1994; Savino et al., 1994a). The overall folding (Nishimura et al., 1996) and ^{1}H, ^{15}N, and ^{13}C assignments (Xu et al., 1996) of human IL-6 have been determined using NMR spectroscopy, showing that IL-6 has the long-chain, four-α-helical bundle structure with up−up−down−down

† This work was supported in part by Australian National Health and Medical Research Council Grants 920528 and 950824.

* Address correspondence to this author at Ludwig Institute for Cancer Research, P.O. 2008, Royal Melbourne Hospital, Parkville, Victoria 3050, Australia. Fax: +61-3-9348-1925. Tel: +61-3-9347-6389. E-mail: simpson@LICRE.ludwig.edu.au.

‡ Ludwig Institute for Cancer Research and the Walter and Eliza Hall Institute of Medical Research.

§ Current address: AMRAD Operations Pty Ltd., Richmond, Victoria 3121, Australia.

|| Biomolecular Research Institute.

⊗ Abstract published in *Advance ACS Abstracts,* April 15, 1997.

[1] Abbreviations: 1D, one dimensional; 2D, two dimensional; CD, circular dichroism; ESI-MS, electrospray ionization mass spectrometry; GdnHCl, guanidine hydrochloride; GH, growth hormone; h, human; IL-6, interleukin-6; IL-6R, interleukin-6 receptor; LIF, leukemia inhibitory factor; m, murine; NMR, nuclear magnetic resonance; NOE, nuclear Overhauser effect; NOESY, 2D nuclear Overhauser effect spectroscopy; PCR, polymerase chain reaction; TOCSY, 2D total correlation spectroscopy.

[2] Note added in proof: A 1.9 Å crystal structure of hIL-6 has been recently reported (Somers et al., 1997).

S0006-2960(96)02939-X CCC: $14.00

topology, as predicted by Bazan (1990), and belongs to the subgroup of long-chain cytokines (Sprang & Bazan, 1993). The determination of the solution structure of murine IL-6 by NMR has been impeded by its tendency to aggregate at high protein concentrations (Morton et al., 1995). In part to establish the cause of this aggregation, a detailed study of the equilibrium unfolding of a recombinant form of murine IL-6 (mIL-6) was performed, which showed that at neutral pH, or in the presence of salt, mIL-6 forms equilibrium unfolding intermediates which aggregate, exhibiting unusual fluorescence characteristics (Ward et al., 1995; Matthews et al., 1996). In terms of their fluorescence properties, these aggregated intermediates and the aggregates formed during NMR studies are identical, the fluorescence quantum yield being enhanced and the emission maximum being blue shifted relative to mIL-6 in its native conformation. The fluorescence emission intensity of mIL-6 is also pH dependent (Ward et al., 1993a), although the conformation of the protein is stable over the pH range 2.0−10.0 (Ward et al., 1993a). There are two tryptophan residues in mIL-6 (Trp34[3] and Trp157) which can contribute to its fluorescence at 295 nm, and the midpoint of fluorescence quenching, pH 6.9, is consistent with the interaction of a histidine residue with one of these tryptophan residues (Ward et al., 1993a). Inspection of the homology model of mIL-6 (Hammacher et al., 1994) shows that His31 and Trp34 are on the solvent-exposed face of helix A in an *i*, *i* + 3 arrangement which could facilitate such an interaction. Taken together, these observations imply that this region of the molecule may contribute to the tendency of mIL-6 to aggregate. Thus, appropriate site-directed mutagenesis in the vicinity of His31 and Trp34 may result in a form of mIL-6 which is more soluble and hence more conducive to NMR solution structure studies.

Residues 31 and 35 in the corresponding region of human IL-6 (hIL-6) have been found recently to be important for biological activity [reviewed by Simpson et al. (1997)]. IL-6 mediates its biological activity by binding to cell surface receptors, triggering a dimerization event which activates signal transduction (Murakami et al., 1993). Intracellular signaling through dimerization of cell surface receptors is also induced by the well-characterized human growth hormone (GH) which is also a member of the long-chain four α-helical bundle cytokine/growth factor family (Wells, 1996). While GH binds to two identical GH receptor molecules (Cunningham et al., 1991; Ultsch et al., 1991), IL-6 binds first to its specific receptor protein, IL-6R (Yamasaki et al., 1988); then this binary complex binds to and activates the transmembrane signal transducer gp130 (Hibi et al., 1990). Using the extracellular domains of the IL-6R and gp130, we (Ward et al., 1994) and others (Paonessa et al., 1995) have shown that the signaling IL-6/receptor complex is hexameric, containing two molecules each of IL-6, IL-6R, and gp130. Although the topology of this ternary complex is not yet known, it is clear that there are three distinct receptor-binding sites on hIL-6 (Simpson et al., 1997). Site I, which binds IL-6R, encompasses part of the A/B loop and the C-terminal end of helix D and corresponds to site I in GH (Kossiakoff et al., 1994). Site II in hIL-6, corresponding to the second receptor-binding site in GH (Kossiakoff et al., 1994), binds gp130 and is composed of residues in the A and C helices. Unlike GH, hIL-6 has a third binding site, site III, which also interacts with gp130 and is formed by residues from the A/B and C/D loops and the N-terminal end of helix D. By homology with hIL-6, His31 and Trp34 form part of site II in mIL-6. Thus, this region of mIL-6, with its fluorescent tryptophan residue, could also be used as a probe for site II binding.

In this study, we have constructed, by site-directed mutagenesis, a series of mIL-6 mutants, H31A, W34A, and H31A/W34A, expressed them in *Escherichia coli*, and purified them to homogeneity for fluorescence spectroscopy, circular dichroism, and equilibrium unfolding studies. Our data show that His31 is responsible for the pH-dependent quenching of fluorescence in mIL-6 and that mutation of Trp34 to alanine reduces the tendency of mIL-6 unfolding intermediates to aggregate and, by extension, reduces the time-dependent aggregation, or "aging" of mIL-6 at high protein concentrations. Furthermore, by NMR methods, we show that His31 and Trp34 interact in mIL-6, albeit with a low energy of interaction.

EXPERIMENTAL PROCEDURES

Materials. Restriction endonucleases were purchased from Boehringer Mannheim (Mannheim, Germany) or New England Biolabs (Beverley, MA). Urea was from Bio-Rad (Richmond, CA). GdnHCl was purchased as an 8 M aqueous stock solution from Pierce (Rockford, IL) or in crystalline form from Mallinckrodt (Paris, KY). ^2H_2O (>99.9% ^2H) and concentrated NaO^2H and ^2HCl were supplied by Cambridge Isotope Laboratories (Cambridge, MA). Buffers were prepared with deionized water purified to 18 MΩ by a tandem Milli-RO and Milli-Q system from Millipore (Bedford, MA).

Construction of mIL-6 Mutants. A truncated form of mIL-6 which lacks 22 N-terminal residues, Δ22-IL-6, was obtained by polymerase chain reaction (PCR) using plasmid p9HP 1B5B12 (Simpson et al., 1988a) as a template with the oligonucleotide primers 5′-CGA CGA ATT CCA CCA CTT CAC AA-3′ (sense) and 5′-TAG TCG ACG GAT CCC TAG GTT TGC CGA-3′ (antisense). The PCR product was subcloned into pBluescript (Stratagene, La Jolla, CA) and excised from pBluescript using *Pvu*II, for blunt end ligation with *Bst*X1 adaptors and subcloning into pCDM8 (Invitrogen Corp.). For the construction of H31A, W34A, and H31A/W34A, the pCDM8 insert was subjected to site-directed mutagenesis using *Escherichia coli* strains BW313 and MC1061/p3 (Invitrogen Corp.) and M13K07 helper phage (Pharmacia, Uppsala, Sweden), essentially as described by Kunkel et al. (1987). The oligonucleotide primers used for the mutagenesis were (1) 5′-GGA GGC TTA ATT ACA GCT GTT CTC TGG GAA AT-3′ (H31A, *Pvu*II site) and (2) 5′-CTT AAT TAC ACA TGT ACT TGG CGG AAA TCG TGG AAA T-3′ (W34A, *Bsr*I site). H31A/W34A was generated using H31A DNA in pCDM8 as a template with primer 2. In addition to the amino acid substitutions, the primers contained unique restriction endonuclease sites to facilitate detection of the mutations. Clones containing the desired mutation were identified by restriction endonuclease mapping. Following restriction endonuclease treatment and agarose gel purification, the mutants were subcloned into *Eco*RI/*Bam*HI digested pUC8 (Pharmacia, Uppsala, Sweden). The constructs were verified by DNA sequencing using an

[3] The numbering described here for the mIL-6 follows the numbering system described for hIL-6 (Simpson et al., 1997).

Applied Biosystems Model 370A DNA sequencer (Foster City, CA). The first eight residues of mIL-6, Thr-Met-Ile-Thr-Pro-Ser-Leu-Ala, and the first five residues of H31A, W34A, and H31A/W34A, Thr-Met-Ile-Asn-Ser, are derived from the N-terminus of bacterial β-galactosidase and the polylinker region of pUC, while the remaining 176 and 165 amino acids correspond to residues 9−184 and 21−184, respectively, of natural mIL-6 with the appropriate mutations at His31 and Trp34 (Simpson et al., 1988a).

Expression and Purification of mIL-6 Mutants. Wild-type recombinant mIL-6 (mIL-6; Simpson et al., 1988a) and H31A, W34A, and H31A/W34A were expressed in *E. coli* strain NM522 and purified to homogeneity as described previously for mIL-6 (Zhang et al., 1992). These proteins were characterized by analytical RP-HPLC, electrospray ionization mass spectrometry (ESI-MS), and N-terminal sequence analysis as described elsewhere (Zhang et al., 1992). The concentration of mIL-6 was determined by amino acid analysis (Simpson et al., 1988b), and the concentrations of H31A, W34A, and H31A/W34A were calculated on the basis of their absorbances at 280 nm in 6 M GdnHCl, as described by Gill and von Hippel (1989). The extinction coefficient for mIL-6 at 280 nm estimated by this method is within 7% of that determined by amino acid analysis. The activity of Δ22-IL-6 is similar to that of mIL-6 (Hammacher et al., 1997) and natural murine IL-6 (Zhang et al., 1992). NMR studies of both mIL-6 and hIL-6 have shown that the N-terminal 22 residues are unstructured (Proudfoot et al., 1993; Morton et al., 1995).

Biological Assay. The biological activities of mIL-6 and derivatives were determined in a mutagenic assay on murine 7TD1 cells as described previously (van Snick et al., 1986; Ward et al., 1993b). Briefly, IL-6-dependent murine hybridoma 7TD1 cells were incubated in a 96-well microtiter plate (2000 cells per microwell), with serial dilutions of the test samples in a total volume of 0.2 mL. Cell growth was determined by assaying succinic dehydrogenase levels using 3-(4,5-dimethylthiazol-2-yl)-2,5-diphenyltetrazolium bromide as a substrate and measuring the absorbance at 560 nm (Mosmann, 1983).

Spectroscopic Measurements. All spectroscopic measurements were made at 25 °C. Circular dichroism measurements were made at 222 nm, with a 0.1 cm path-length cell and protein concentrations of 100 μg/mL, using an Aviv Model 62DS (Lakewood, NJ) CD spectrometer. Fluorescence data were collected on a Perkin-Elmer Model LS5 luminescence spectrophotometer using 0.5 cm path-length cells at 25 °C and 5 nm emission slit widths. Excitation wavelengths were 295 nm to preferentially excite tryptophan side chains. Protein concentrations were 30 μg/mL.

Denaturant-Induced Unfolding. Urea- and GdnHCl-induced unfolding of mIL-6 and mutants was monitored by the changes in the CD signal at 222 nm or fluorescence (emission intensity at 345 nm and λ_{max} in the range 310−400 nm) as a function of denaturant concentration in either 10 mM Tris-HCl, pH 7.4, or 10 mM sodium acetate, pH 4.0 (Ward et al., 1995). Protein concentrations were 0.1 mg/mL. Solutions were incubated at 25 °C for 14 h prior to measurement.

Analysis of Equilibrium Unfolding Data. Two-state unfolding involves a sharp transition between the folded and unfolded states of a protein, F ↔ U, where these species are the only two present. Non-two-state unfolding involves the presence of one species intermediate or more to the folded and unfolded states, F ↔ I ↔ U. For a two-state unfolding process, the free energy of unfolding, ΔG_{unf}, is related to the denaturant concentration at the midpoint of unfolding, $[D]_{50\%}$, according to the relationship $\Delta G_{unf} = m[D]_{50\%}$, where m is the slope of the unfolding curve in the transition region. m is a measure of the sharpness of the unfolding transition and can be used as an approximate indicator of the two-state nature of unfolding. When S is the measured property of the protein at a given denaturant (D) concentration, unfolding data can be analyzed according to the equation

$$S = \frac{F(S_N + S_U \exp(A))}{1 + \exp(A)} \quad (1)$$

where $A = \{m[D] - \Delta G_{unf}\}/RT = m([D] - [D]_{50\%})/RT$ (Santoro & Bolen, 1986; Clarke & Fersht, 1993). N is the native state, U is the unfolded state, R is the gas constant, and T is absolute temperature. When there are pre- or posttransitional baseline dependencies on denaturant concentration, S_N and S_U are replaced by $S_N - a[D]$ and $S_U - b[D]$, where a and b are the slopes of the pre- and posttransitional baselines, respectively. Where appropriate, data were fitted using the nonlinear regression analysis program KaleidaGraph (version 3.0 Synergy Software; PCS Inc.).

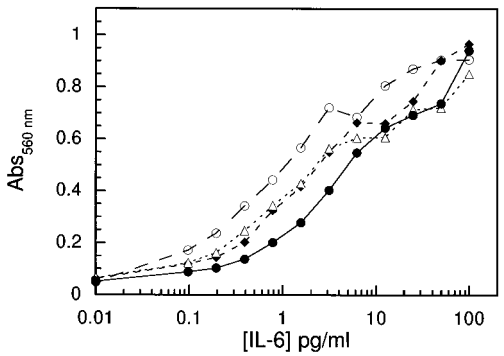

FIGURE 1: Biological activity of mIL-6 (◆), H31A (△), W34A (○), and H31A/W34A (●) using 7TD1 cells. Cell growth was determined by assaying succinic dehydrogenase levels using 3-(4,5-dimethylthiazol-2-yl)-2,5-diphenyltetrazolium bromide as a substrate and measuring the absorbance at 560 nm. Each point represents the average of three separate measurements in a representative experiment. Separate experiments show the same results, with similar scatter of results but different order of mitogenic activity among the four proteins.

Nuclear Magnetic Resonance (NMR) Spectroscopy. Samples for NMR spectroscopy were prepared by dissolving lyophilized protein in 500 μL of either ^2H_2O or 90% H_2O/10% ^2H_2O. ^1H NMR spectra were recorded on Bruker AMX-600 and -500 spectrometers. The probe temperature was maintained at 20 °C using a B-VT1000E control unit and a Haake cooling bath. In all experiments the carrier was set in the center of the spectrum, and quadrature detection was used in both dimensions. Solvent suppression was carried out by selective, low-power irradiation of the water resonance during the relaxation delay (typically 1.5−2.0 s) and, in NOESY experiments, also during the mixing time. All 2D spectra were recorded the in phase-sensitive mode using the time-proportional phase incrementation method (Marion & Wüthrich, 1983). Two-dimensional TOCSY experiments (Braunschweiler & Ernst, 1983) were recorded using the DIPSI-2 (Rucker & Shaka, 1989) spin-

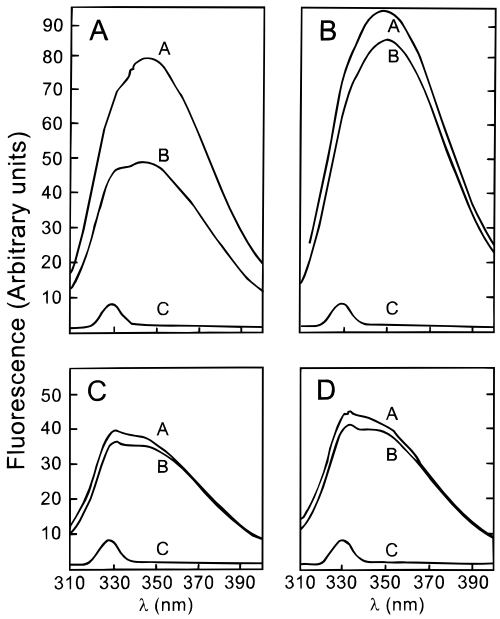

FIGURE 2: Fluorescence spectra of mIL-6 (panel A), H31A (panel B), W34A (panel C), and H31A/W34A (panel D). In each panel, spectrum A is the fluorescence at pH 7.4 (buffer: 10 mM Tris-HCl), spectrum B is the fluorescence at pH 4.0 (buffer: 10 mM sodium acetate), and spectrum C is the baseline fluorescence, which was identical for both buffers used. Protein concentrations were 30 μg/mL, the excitation wavelength was 295 nm, and emission was scanned from 310 to 400 nm in 1 nm steps. All spectra were recorded on the same day and are directly comparable with respect to scale.

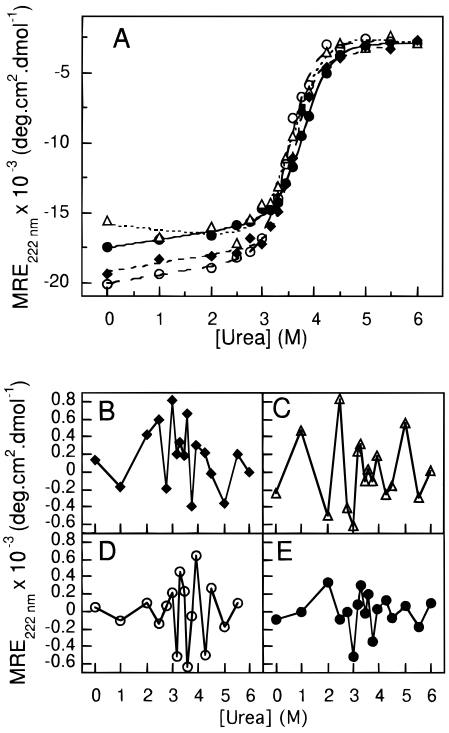

FIGURE 3: Equilibrium urea-induced unfolding at pH 4.0 of mIL-6 (◆), H31A (△), W34A (○) and H31A/W34A (●) monitored by CD at 222 nm. Data are presented in terms of mean residue ellipticity (MRE) and were fitted to eq 1 using a pre- and posttransitional baseline dependence of signal on denaturant concentration, and the residuals of each fit are shown in panels B, C, D, and E, respectively.

lock sequence, with mixing times of 32−35 ms. Two-dimensional NOESY spectra (Anil Kumar et al., 1980; Macura et al., 1981) were recorded with a mixing time of 140 ms. Typically, 400−500 t_1 increments were acquired, with 160−176 scans per increment and 4K data points per increment. For 2D spectra (all recorded at 600.14 MHz) sweep widths were 7143 Hz for samples in ^2H_2O and 7353 Hz for samples in H_2O. 1D spectra were acquired over 8K data points, with sweep widths as for 2D spectra at 600 MHz, and 5208 Hz at 500 MHz.

Spectra were processed and analyzed on Silicon Graphics IRIS 4D/30 workstations using FELIX (versions 1.1 and 2.05, from Hare Research Inc., Bothell, WA). Before Fourier transformation, phase-shifted (50−70°), skewed, sine-squared window functions were applied to 2D spectra, and Lorentzian-to-Gaussian window functions were applied to 1D spectra. Where necessary, spectra were subjected to baseline correction and t_1 noise suppression (Manoleras & Norton, 1992). Aromatic chemical shifts obtained from 2D spectra were measured from NOESY spectra of the protein in ^2H_2O, except for the indole N(1)H resonances, which were measured from NOESY spectra in H_2O.

pH Measurement and Titrations for NMR Experiments. The pH was adjusted with 0.1 M ^{2}HCl or NaO^{2}H and measured at 22 °C both before and after NMR experiments with an Activon Model 209 pH meter and an Ingold 6030-02 microelectrode. pH readings were not adjusted for deuterium isotope effects. Protein concentrations for 2D NMR were *ca.* 1 mM. Chemical shifts are referenced to 2,2-dimethyl-2-silapentane-5-sulfonate. pK_a values were obtained by nonlinear least squares fits of the observed chemical shifts as a function of pH to the Henderson−Hasselbach equation for a single ionization, assuming fast exchange between the conjugate acids and bases.

Model Building of Helix A. A structural model for residues 28−37 of mIL-6 was generated using the Biopolymer module of InsightII (version 2.3.0, Biosym Technologies, San Diego, CA). An α-helical conformation as predicted by Bazan (1990) was specified; then the orientations of the His31 and Trp34 side chains were manipulated manually by rotations about their $C^\alpha-C^\beta$ and $C^\beta-C^\gamma$ bonds to produce a conformation consistent with the observed NOE connectivities between them, and the structure was subjected to unrestrained conjugate-gradient energy minimization in the Discover module using the CVFF force field *in vacuo*. InsightII was also used to produce Figure 8.

RESULTS

Biological Activity. The biological activities of mIL-6, H31A, W34A, and H31A/W34A were tested using a mitogenic assay on 7TD1 cells. Within the limits of the experiment, the activities of all four proteins are indistinguishable (Figure 1).

Fluorescence Spectra of mIL-6 and Mutant Proteins. Fluorescence spectra of the proteins were measured at pH 4.0 and 7.4 (Figure 2). As can be seen in Figure 2A, the fluorescence of mIL-6 at pH 4.0 (spectrum B) is only 60% that of the fluorescence at pH 7.4 (spectrum A). For H31A (Figure 2B) the fluorescence at pH 4.0 (spectrum B) has increased to become approximately 90% of the fluorescence at pH 7.4 (spectrum A), which is 15% higher than that of mIL-6 at pH 7.4. For both W34A (Figure 2C) and H31A/W34A (Figure 2D), the fluorescence at both pH 7.4 (spectra A) and pH 4.0 (spectra B), which is mainly due to Trp157, is less than half that of the unquenched fluorescence when

Table 1: Equilibrium Unfolding of mIL-6 Proteins[a]

denaturing conditions	protein	$[D]_{50\%}$ (M)	m (kcal·mol^{-1}·M^{-1})	ΔG_{unf} (kcal·mol^{-1})
pH 4.0, urea	mIL-6	3.59 ± 0.02	3.0 ± 0.3	10.8 ± 1.1
	H31A	3.58 ± 0.05	1.9 ± 0.3	6.9 ± 0.9
	W34A	3.50 ± 0.03	2.5 ± 0.3	8.8 ± 1.0
	H31A/W34A	3.80 ± 0.03	2.3 ± 0.2	8.6 ± 0.7
pH 7.4, urea[b]	mIL-6	5.2 ± 0.2	1.1 ± 0.3	5.7 ± 1.7
	W34A	4.6 ± 0.1	1.0 ± 0.1	4.0 ± 1.0
	H31A/W34A	4.9 ± 0.1	1.5 ± 0.2	7.5 ± 0.9
pH 7.4, GdnHCl[c]	mIL-6	1.9 ± 0.1	1.0 ± 0.2	1.9 ± 0.3
	H31A	2.0 ± 0.3	0.8 ± 0.3	1.6 ± 0.6
	W34A	1.98 ± 0.04	2.5 ± 0.4	5.0 ± 0.8
	H31A/W34A	2.00 ± 0.03	3.0 ± 0.5	6.0 ± 1.0

[a] Values were obtained by fitting unfolding data to eq 1 with pre- and posttransitional dependence of signal on denaturant concentration. Tolerances shown are due to fitting errors. [b] Data for urea denaturation of H31A at pH 7.4 could not be fitted to eq 1 with pre- and posttransitional dependence of signal on denaturant concentration. [c] Data were fitted to eq 1 with posttransitional dependence of signal on denaturant concentration only.

Trp34 is present (Figure 2A, spectrum A; Figure 2B, spectra A and B) and only marginally less than that of mIL-6 at pH 4, where fluorescence is quenched (Figure 2A, spectrum B). For both these mutants the fluorescence at pH 4.0 (spectra B) is approximately 90% that at pH 7.4 (spectra A).

Equilibrium Unfolding at pH 4.0 and 7.4. The stability of the proteins was determined at 25 °C by urea denaturation at pH 4.0, using CD to monitor the change in signal at 222 nm, and the data were analyzed using eq 1 (Figure 3A, Table 1). The most reliable parameter for stability differences in this study is $[D]_{50\%}$, the denaturant concentration at the midpoint of unfolding. Under these conditions mIL-6, H31A, and W34A have very similar values of $[D]_{50\%}$, while H31A/W34A is marginally more stable, having a higher value of $[D]_{50\%}$. Values of ΔG_{unf} are more dispersed, with W34A, H31A/W34A, and H31A being less stable than mIL-6 by 2.2 ± 1.3, 2.0 ± 1.5, and 4.0 ± 1.4 kcal/mol, respectively. These different stabilities result from the different m values for each unfolding curve. Although m is the parameter most susceptible to experimental variance, the much lower value of m for H31A compared with mIL-6 (Table 1) indicates that the unfolding of this protein is most likely to deviate from a two-state unfolding mechanism. Inspection of the residuals for the fit of the data to eq 1 (Figure 3B−E) shows that the data for H31A have a scatter similar to that of mIL-6. Only H31A/W34A shows an appreciably better fit to eq 1 and a two-state unfolding mechanism (Figure 3E).

The unfolding of these proteins as monitored by far-UV CD was also performed at pH 7.4, using both urea and GdnHCl as denaturants. In the presence of GdnHCl (Figure 4A, Table 1), mIL-6 and H31A have similar unfolding properties. With increasing concentrations of GdnHCl, the CD signals gradually decrease to 50% at 2 M GdnHCl, followed by a sharper unfolding phase from 2 to 2.5 M GdnHCl. In contrast, the tryptophan mutants, W34A and H31A/W34A, appear to have a single unfolding transition. Values of $[D]_{50\%}$ are not significantly different, but the values of m and thus ΔG_{unf} as estimated from eq 1 for these mutants are up to 3-fold greater than those of mIL-6 and H31A (Table 1). Inspection of the residuals of the fit (inset panels) in each case shows a better fit to eq 1 for W34A and H31A/W34A. This indicates that under these conditions the unfolding of W34A and H31A/W34A is closer to a two-state unfolding transition than both mIL-6 and H31A. When urea is used as the denaturant, the unfolding data for mIL-6 and H31A (Figure 4B, Table 1) again show a more gradual decrease in signal than the sharper unfolding transitions of W34A and H31A/W34A (Figure 4C, Table 1). Under these conditions, however, the differences between the four proteins are more distinct. H31A shows larger residuals and behaves less well than mIL-6, while the H31A/W34A, with the highest value of m, smallest residuals, and sharpest unfolding transition, has the most two-state-like unfolding behavior.

GdnHCl-Induced Unfolding Monitored by Fluorescence at pH 4.0. The equilibrium unfolding of the proteins was also carried out at pH 4.0 using GdnHCl as the denaturant and monitored using fluorescence. The fluorescence behavior of mIL-6 in GdnHCl at pH 4.0 has been described previously (Ward et al., 1995; Matthews et al., 1996). Both fluorescence emission intensity and λ_{max} show a biphasic unfolding transition which is consistent with the aggregation of partially unfolded forms of mIL-6 at low to intermediate denaturant concentrations, followed by complete unfolding at higher denaturant concentrations (Figure 5A). The fluorescence behavior of H31A (Figure 5B) shows high fluorescence emission intensity at low to moderate denaturant concentrations, consistent with the removal of the quenching histidine side chain. Beyond 3.5 M GdnHCl there is a small decrease in fluorescence intensity accompanied by a red shift of λ_{max} which is typical for the global unfolding of a protein (Lakowicz, 1983). There is a blue shift of λ_{max} at low GdnHCl (<1 M GdnHCl) to a minimum at much lower concentrations than the similar blue shift of λ_{max} observed with mIL-6, signifying aggregation of the early unfolding intermediates at very low concentrations of the ionic denaturant. The tryptophan mutants W34A and H31A/W34A (Figure 5C,D) both have a low intrinsic fluorescence with no significant changes of intensity at 345 nm over the full range of denaturant concentration. The λ_{max} for these proteins shows no blue shift at low to moderate concentrations of denaturant but does exhibit the red shift typical of unfolding at moderate denaturant concentrations. This confirms that the unusual fluorescence behavior shown by mIL-6 on unfolding is due to Trp34 and not to Trp157. It does not, however, indicate the absence of unfolding intermediates in W34A and H31A/W34A. When far UV-CD is used to monitor unfolding under these conditions, all four proteins exhibit non-monophasic unfolding profiles which indicate the presence of intermediates (Figure 5). Here only W34A has a sharper unfolding transition than mIL-6 (Figure 5C), while the scattered data for H31A are consistent with a high degree of aggregation.

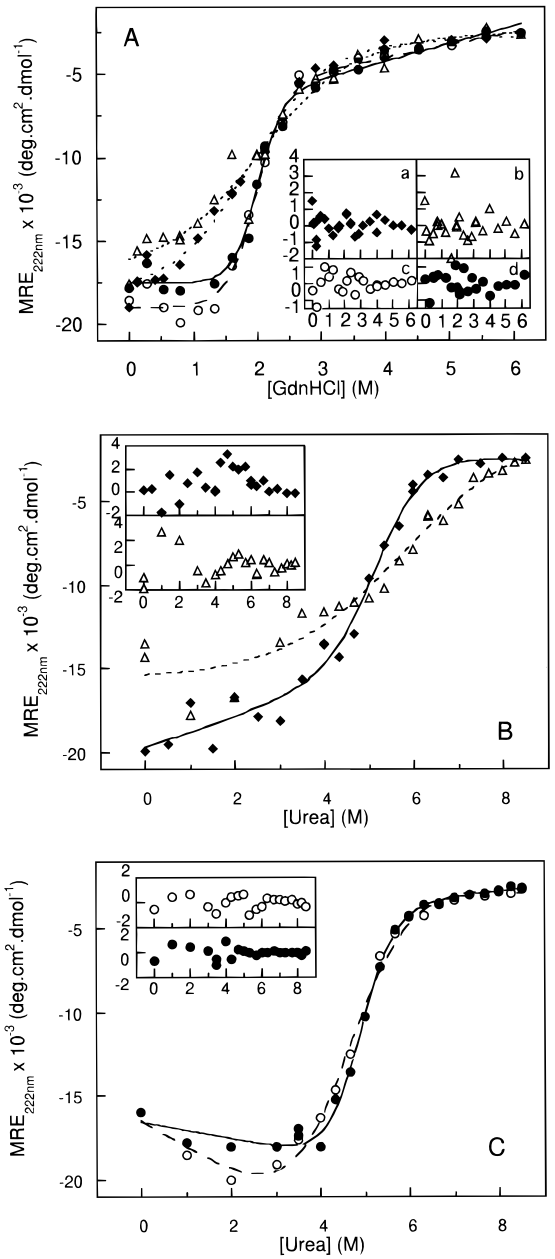

FIGURE 4: Equilibrium urea-induced unfolding of mIL-6 (◆), H31A (△), W34A (○), and H31A/W34A (●) monitored by CD at pH 7.4. Data are presented in terms of mean residue ellipticity (MRE). Panel A shows GdnHCl denaturation, and data are fitted to eq 1 using only a posttransitional dependence of signal on denaturant concentration. The residuals of each fit are shown in the inset panels: a (mIL-6), b (H31A), c (W34A), and d (H31A/W34A). Panel B shows the urea denaturation of mIL-6 and H31A, and panel C shows the urea denaturation of W34A, and H31A/W34A. Data for mIL-6, W34A and H31A/W34A were fitted to eq 1 with a pre- and posttransitional baseline dependence of signal on denaturant concentration. Data for H31A were fitted to eq 1 with no pre- and posttransitional dependence of signal on denaturant concentration. Residuals for each fit are shown in the inset panels using the same symbols as in the main panels.

In NMR experiments conducted at high protein concentrations (10−20 mg/mL) at pH 3.5−4, H31A was more prone to aggregation, and W34A less so, compared with mIL-6. These findings concur with our observations of intermediate formation and aggregation.

NMR Spectroscopy. The ^{1}H chemical shifts of all aromatic spin systems in mIL-6 were reported by Morton et al. (1995) although only one unequivocal sequence-specific assignment was made. The chemical shifts of the N-terminally truncated mIL-6 used in the present study were essentially identical to those of Morton et al. (1995), emphasizing the insensitivity of the bulk of the structure to deletion of the N-terminal 22 residues. The exception is the spin system of Tyr20 [TyrE in the nomenclature of Morton et al. (1995)], which is missing in mIL-6 used in this study.

In H31A and W34A the chemical shifts of all aromatic resonances, except those of the mutated residues, were within 0.03 ppm (in most cases 0.01 ppm) of corresponding values in mIL-6, indicating that the overall conformation of the protein was not significantly disrupted in either case. This conclusion was supported by inspection of the upfield regions of the 1D NMR spectra of these proteins, which contain resonances from aliphatic protons close to aromatic groups (Ward et al., 1993b; Morton et al., 1995) and which were similar to the spectrum of mIL-6 (Figure 6). The spectrum of H31A (Figure 6C) showed minor chemical shift differences from that of mIL-6, and its resonances were slightly broader, consistent with its greater tendency to aggregate. The downfield region of the spectrum of W34A (Figure 6B) showed clearly that, of the two indole NH resonances around 10−10.3 ppm in the native spectrum (Figure 6A), the further upfield and sharper peak arose from Trp34.

As noted previously (Morton et al., 1995), there are NOEs between the aromatic protons of a histidine and a tryptophan residue. Given that His31 and Trp34 are in a region of the molecule predicted to be helical (Bazan, 1990), it was expected that the residues involved would be His31 and Trp34. The alanine substitutions of His31 and Trp34 made in this work confirm that this is the case (Figure 6), providing firm assignments for these two spin systems. Comparison of the spectra of mIL-6, H31A, and W34A also allows the aliphatic resonances of these two residues to be assigned, as follows: His31 $C^{\alpha}H$ 4.64, $C^{\beta}H$ 3.38, 3.59; Trp34 $C^{\alpha}H$ 4.30, $C^{\beta}H$ 3.38, 3.64 (backbone NH tentatively at 7.77 ppm).

The imidazolium pK_a of His31 was unremarkable in mIL-6 (pK_a = 6.5) but increased by 0.3 unit in W34A. The pK_a values of two of the other three histidine side chains were unchanged in the H31A and W34A. The final histidine side chain has a low pK_a in mIL-6 and H31A (pK_a = 5.5) and showed a minor increase in W34A (pK_a = 5.6).

Figure 7 shows the region of a NOESY spectrum of IL-6 in ^2H_2O containing connectivities between the C(2)H resonance of His31 and C(4)H, C(5)H, and C(6)H of Trp34. His C(2)H to C(4)H NOEs are also observed for His31 and two other histidines [B and C using the nomenclature of Morton et al. (1995)]. Because the $C^{\beta}H$ resonances of His31 and Trp34 had similar chemical shifts (in fact both residues have one $C^{\beta}H$ resonance at 3.38 ppm), it was not clear if there were interresidue aromatic to $C^{\beta}H$ NOEs. Nevertheless, as shown in Figure 8, it is possible to orient these two side chains in a way which agrees with the relative intensities of the aromatic−aromatic NOEs and the lack of NOEs from Trp34 to C(4)H of His31 and is consistent with helical structure in this region, as predicted by Bazan (1990). However, it must be emphasized that this is a model based on limited data and that in the IL-6 structure the helix may be slightly curved. The indole NH resonance of Trp34 is sharper than that of Trp157 (Figures 6 and 7), consistent with a greater mobility and/or a smaller number of nearby protons for Trp34, also reflecting its location on the surface of the protein.

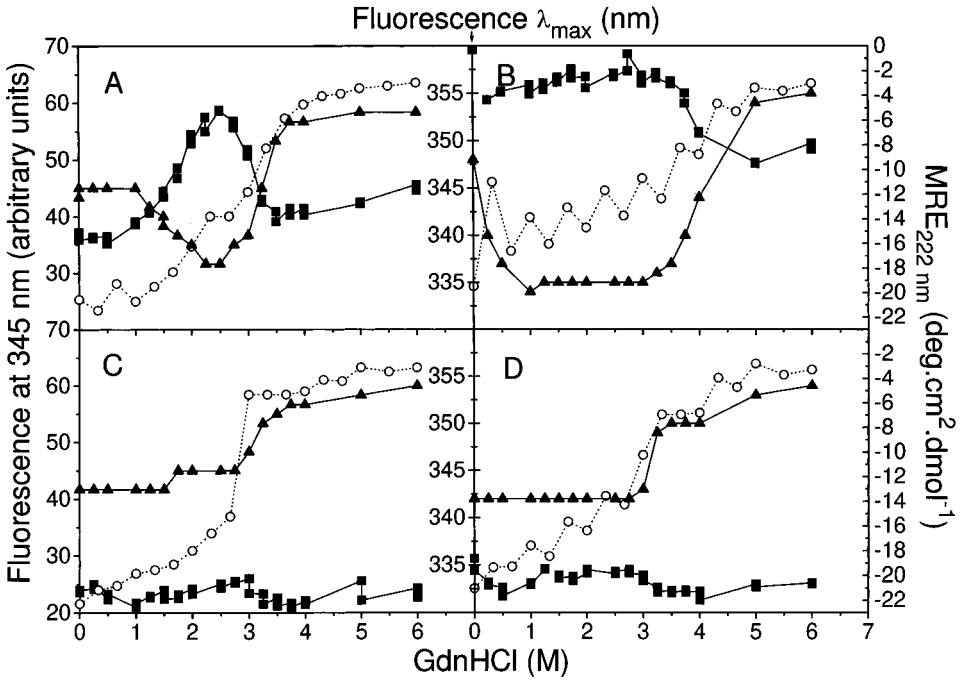

FIGURE 5: Equilibrium GdnHCl-induced unfolding of mIL-6 (panel A), H31A (panel B), W34A (panel C), and H31A/W34A (panel D) monitored by fluorescence and CD at pH 4.0. Fluorescence emission intensities at 345 nm (■), left-hand abscissa; wavelength maxima (▲), middle abscissa; CD signal at 222 nm (○), right-hand abscissa, presented in terms of mean residue ellipticity (MRE). Data are presented as line diagrams and are not fitted to any equation.

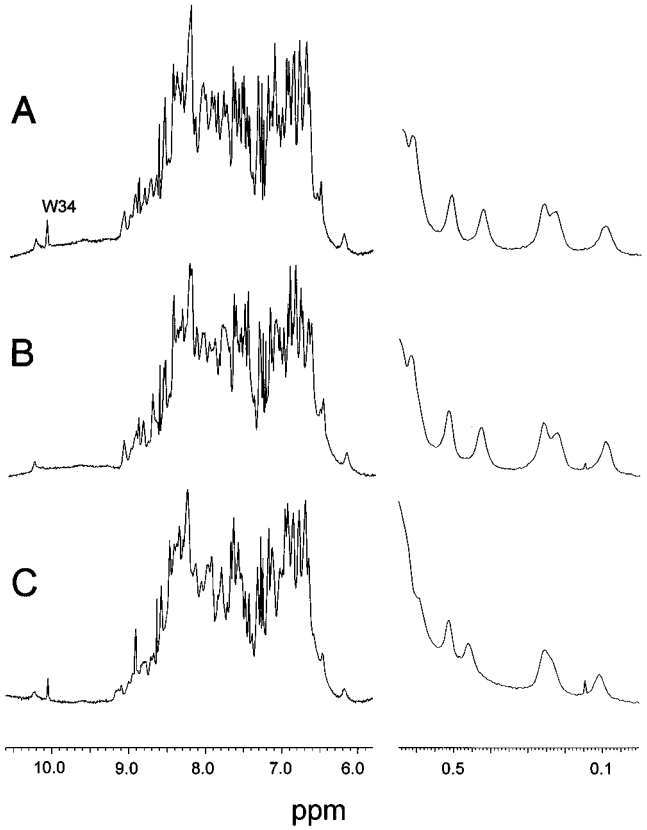

FIGURE 6: 1D ^{1}H NMR spectra at 600 MHz in 90% H_2O/10% ^2H_2O, pH 3.5, at 20 °C: (A) mIL-6; (B) W34A; (C) H31A. Left-hand panels show the aromatic/amide regions and right-hand panels show the upfield methyl regions. Vertical scales are different in each case. The indole NH resonance of Trp34 at 10.1 ppm is labeled. The small sharp peak at 0.15 ppm results from an impurity.

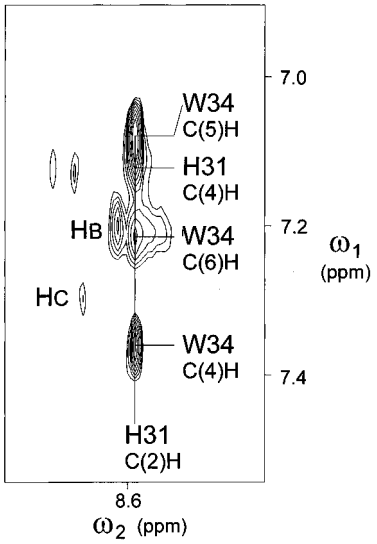

FIGURE 7: Region of a NOESY spectrum of mIL-6, in ^2H_2O at pH 3.5 and 20 °C, showing connectivities between the aromatic resonances of His31 and Trp34. The peaks labeled HB and HC represent the C(2)H to C(4)H NOEs for two other histidine residues.

Ring current shift interactions (Case, 1995) between His31 and Trp34 are relatively weak. When Trp34 was replaced with alanine, the chemical shifts of the C(2)H and C(4)H resonances of His31 changed by ≤0.04 ppm. In H31A the only significant changes were for C(4)H and C(5)H, which moved downfield by 0.30 and 0.07 ppm, respectively. These changes are qualitatively consistent with the structure shown in Figure 8 where the edge of the indole ring is oriented toward the face of His31. At the pH of the NMR measurements His31 is protonated, so replacement with Ala also removed a nearby positive charge. The observed changes in the Trp34 chemical shifts in H31A, however, were in the opposite direction to those expected for removal of an electrostatic interaction, suggesting that the actual ring current effects of His31 on the C(4)H and C(5)H resonances of Trp34 were slightly larger than the observed differences in H31A.

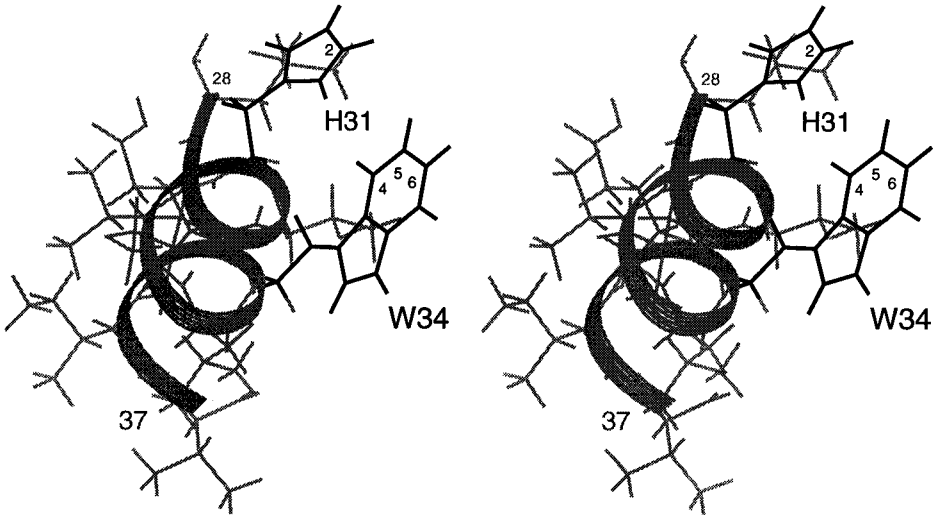

FIGURE 8: Stereoview of a model of residues 28−37 of mIL-6 in an α-helical conformation [as predicted by Bazan (1990)], showing the side chains of His31 and Trp34 in a conformation consistent with the observed NOE connectivities between them.

DISCUSSION

Previously, we described the pH-dependent quenching of fluorescence (Ward et al., 1993a) and the unusual fluorescence behavior of mIL-6 during denaturant-induced, equilibrium unfolding in the presence of salt (Ward et al., 1995). The selective mutation of His31 to alanine eliminates this pH-dependent quenching of mIL-6 (Figures 2B and 5B). Similarly, the pH dependence of the signal intensity is eliminated in both W34A and H31A/W34A, and as expected for the removal of a tryptophan residue, the fluorescence emission intensities of these mutants are 2-fold less than those of mIL-6 and H31A. These observations confirm that His31 is responsible for the pH-dependent quenching of Trp34 in mIL-6. The fluorescence behavior of the mIL-6 mutants during equilibrium unfolding is also altered. We had proposed that the increase of the fluorescence emission signal and concomitant blue shift of λ_{max} at low to moderate denaturant concentrations were due to the association of partially unfolded intermediate states of mIL-6, whereas the decrease of the fluorescence emission signal and concomitant red shift of λ_{max} at moderate to high denaturant concentrations were due to the dissociation and unfolding of these intermediate states (Ward et al., 1995). For the Trp34 mutants the initial increase of the fluorescence emission signal and blue shift of λ_{max} are no longer observed, confirming that the unusual fluorescence behavior originated from Trp34. In contrast, the blue shift in λ_{max} in H31A occurs at relatively lower denaturant concentrations than for mIL-6, indicating that intermediate formation and aggregation are occurring more readily for this mutant. The CD-monitored experiments show that the unfolding behavior of H31A tends to deviate from two-state behavior to a greater extent than for mIL-6, while that of W34A and more particularly H31A/W34A approaches two-state unfolding. All of these observations strongly implicate the region encompassing His31 and Trp34 as being involved in the formation and association of equilibrium unfolding intermediates. The increased tendency to form equilibrium unfolding intermediates corresponds to an increased tendency to aggregate at high concentrations during NMR experiments.

The side chains in the primary sequence of mIL-6 N-terminal from His31 and Trp34 are uncharged, whereas

hIL-6 numbering	25	26	27	28	29	30	31	32	33	34	35	36	37	38	39	40	41	42
*fully conserved residue					*							*						*
consensus sequence	-	E	-	L	I	K	Y	I	L	-	K	I	S	A	L	R	K	E
hIL-6	I	D	K	Q	I	R	Y	I	L	D	G	I	S	A	L	R	K	E
mIL-6	V	G	G	L	I	T	H	V	L	W	E	I	V	E	M	R	K	E

FIGURE 9: Sequence comparison of mIL-6, hIL-6, and a consensus sequence on 11 full sequences and 1 partial sequence of IL-6 from different species (Simpson et al., 1997) spanning residues 25−42. Residues corresponding to His31 and Trp34 are boxed.

the equivalent residues of other known IL-6 species contain charged residues (Figure 9). This lack of charge makes this region a potentially "sticky" patch in mIL-6, while the presence of an adjacent pair of glycine residues, traditionally thought of as having a low propensity to form α-helices (Chou & Fasman, 1978), may cause the A helix to unravel at relatively low concentrations of denaturant. Therefore, these features further implicate the region close to His31 and Trp34 as being involved in the association of partially unfolded states of mIL-6. This effect would be amplified at neutral pH, where His31 is deprotonated, causing the histidine side chain to become more hydrophobic in nature, and removing a potential *i*, *i* + *4* stabilizing electrostatic interaction between His31 and Glu35. The double mutation of His31 and Trp34 to alanine removes two surface hydrophobic side chains and reduces the association tendencies of the protein. The introduction of permanently charged side chains by site-directed mutagenesis may further reduce these effects.

The His31−Trp34 Interaction. It has been reported that, in protein crystal structures, aromatic residues have a tendency to be near His residues and that His−aromatic interactions play a role in stabilizing protein structure or influencing protein function (Loewenthal et al., 1992). For example, in structural terms, His−aromatic interactions are found in antigen−antibody complexes (Anglister & Zilber, 1990), zinc fingers (Kochoyan et al., 1991; Jasanoff & Weiss, 1993), and active sites of enzymes (Ito et al., 1991; Wery et al., 1991). In terms of protein stability, Loewenthal et al. (1992) found that the interaction between protonated His18 and Trp94 in barnase provided 1.4 kcal/mol of stability, whereas the nonprotonated His18−Trp94 interaction provided only 0.4 kcal/mol of stability. More recently, studies

on pairwise interactions in α-helices have been performed. Creamer and Rose (1995), making calculations of a model 19-residue polyalanyl α-helix, estimated that an *i, i + 3* histidine−tryptophan interaction would be marginally destabilizing (0.27 kcal/mol). In contrast, Muñoz and Serrano (1994), using an empirical analysis of experimental NMR data of α-helical peptides based on protein sequences, estimated that the same interaction would be marginally stabilizing (0.3 kcal/mol). These discrepancies probably arise from the use of nonprotonated histidine in the first instance and protonated histidine in the second.

The strength of an interaction between two side chains, Δ^2G_{int}, can be estimated using site-directed mutagenesis and double-mutant cycle analysis (Horovitz & Fersht, 1992). Using this method we can make a rough estimate of the stabilizing effect of the His31 and Trp34 side chain−side chain interaction, based on $[urea]_{50\%}$ values at pH 4.0, as 0.20 ± 0.08 M, or 0.4−0.6 kcal/mol. This fairly low interaction energy is consistent with that predicted by Muñoz and Serrano (1994) for an *i, i + 3* configuration on the solvent-exposed face of helix A.

Our NMR data are consistent with the *i, i + 3* interaction between His31 and Trp34 (Figure 8). The increase of the imidazolium pK_a by 0.3 unit in W34A is opposite to that which would have been expected by analogy with the His18−Trp94 interaction in barnase (Loewenthal et al., 1992), where substitution of Trp94 by Leu caused a 0.6 unit decrease in the pK_a. In that case, the centers of the two side chain rings are separated by 4.0 Å and at an angle of 43°. In mIL-6, however, the relative orientation of the two aromatic rings is such that favorable interactions which could stabilize the imidazolium form of His31 are not significant, in agreement with our estimation of a low interaction energy between His31 and Trp34. The increase of pK_a on the substitution of Ala for Trp34 suggests that His31 is able to make new interactions which stabilize its charged form, for example, with the carboxylate side chain of Glu35.

Implications of Mutation in Site II. In hIL-6, specific mutations (Y31D and G35F) in site II, a gp130 binding region, decreased biological activity, although other (including some very radical) mutations had little or no effect on biological activity (Savino et al., 1994a). Residues His31 and Trp34 in mIL-6 correspond to Tyr31 and Asp34 in hIL-6 and may form part of site II based on the assumption that the binding sites are similar for mIL-6. We showed that the mutation of His31 and Trp34 to alanine, both singly and in combination, had no significant effect on biological activity. However, this does not exclude the that fact His31 and Trp34 form part of site II in mIL-6. For example, only a fraction of the residues which form part of site I on hGH have been shown to be important for binding (8 out of 31 side chains account for 85% of the binding energy; Clackson & Wells, 1995). Furthermore, although mIL-6 will only bind to the mouse IL-6R, hIL-6 binds to both the mouse and the human IL-6R (Coulie et al., 1989). This indicates some flexibility in the requirements of the IL-6R for binding site I residues. This flexibility is also noted in the hGH. Essentially identical residues in each of the two hGH receptor molecules interact with different sites (sites I and II) on hGH (deVos et al., 1992), while the prolactin receptor, which is closely related to the GH receptor, in primary sequence and structure, uses a correspondingly different set of residues to interact with hGH only at site I (Kossiakoff et al., 1994). Such apparent flexibility would allow for mutation to smaller side chains of noncritical residues in the putative site II in mIL-6 (e.g., His31 and Trp34) to be made without any effect on binding or activity. Conversely, the radical mutations Y31D (aromatic to negatively charged) and G35F (small to large aromatic side chain) in site II of hIL-6 (Savino et al., 1994a,b) probably prevent the correct positioning of gp130 and/or the IL-6R due to electrostatic and steric effects. Similarly, radical mutations of residues close to His31 and Trp34 in mIL-6 would be predicted to have deleterious effects on activity.

In summary, we have shown that His31 and Trp34 interact with one another in mIL-6, but that this interaction makes only a small contribution to the protein's stability. These residues are responsible for the pH-dependent fluorescence of the protein and are at least partially responsible for the aggregation of partially unfolded intermediates of mIL-6. Further mutation in this region should yield forms of mIL-6 even less prone to aggregation, which would be suitable for NMR studies and may identify residues important for the IL-6R-dependent binding of mIL-6 to gp130.

ACKNOWLEDGMENT

We thank A. W. Burgess for critical review of the manuscript. We also thank R. L. Moritz for providing the purified proteins used in this study, G. E. Reid for ESI-MS analysis, G.-F. Tu for DNA sequencing, J. Weinstock for the mitogenic assays, and T. R. Dyke for assistance with some of the NMR measurements.

REFERENCES

Akira, S., Taga, T., & Kishimoto, T. (1993) *Adv. Immunol. 54*, 1−78.
Anglister, J., & Zilber, B. (1990) *Biochemistry 29*, 921−928.
Anil Kumar, Ernst, R. R., & Wüthrich, K. (1980) *Biochem. Biophys. Res. Commun. 95*, 1−6.
Bazan, J. F. (1990) *Immunol. Today 11*, 350−354.
Braunschweiler, L., & Ernst, R. R. (1983) *J. Magn. Reson. 53*, 521−528.
Case, D. A. (1995) *J. Biomol. NMR 6*, 341−346.
Chou, P. Y., & Fasman, G. D. (1978) *Annu. Rev. Biochem. 47*, 251−276.
Clackson, T., & Wells, J. A. (1995) *Science 267*, 383−386.
Clarke, J., & Fersht, A. R. (1993) *Biochemistry 32*, 4322−4329.
Coulie, P. G., Stephens, M., & van Snick, J. (1989) *Eur. J. Immunol. 19*, 2107−2114.
Creamer, T. P., & Rose, G. D. (1995) *Protein Sci. 4*, 1305−1314.
Cunningham, B. C., Ultsch, M., de Vos, A. M., Mulkerrin, M. G., Clauser, K. R., & Wells, J. A. (1991) *Science 254*, 821−825.
deVos, A. M., Ultsch, M., & Kossiakoff, A. A. (1992) *Science 255*, 306−312.
Ehlers, M., Grötzinger, J., de Hon, F. D., Müllberg, J., Brakenhoff, J. P. J., Liu, J., Wollmer, A., & Rose-John, S. (1994) *J. Immunol. 153*, 1744−1753.
Gill, S. G., & von Hippel, P. H. (1989) *Anal. Biochem. 182*, 319−326.
Hammacher, A., Ward, L. D., Weinstock, J., Treutlein, H., Yasukawa, K., & Simpson, R. J. (1994) *Protein Sci. 3*, 2280−2293.
Hammacher, A., Reid, G. E., Moritz, R. L., & Simpson, R. J. (1997) *Biomed. Chromatogr*. (in press).
Hibi, M., Murakami, M., Saito, M., Hirano, T., Taga, T., & Kishimoto, T. (1990) *Cell 63*, 1149−1157.
Hill, C. P., Osslund, T. D., & Eisenberg, D. (1993) *Proc. Natl. Acad. Sci. U.S.A. 90*, 5167−5171.
Hirano, T. (1994) in *The cytokine handbook* (Thomson, A., Ed.) 2nd ed., pp 145−167, Academic Press, New York.
Horovitz, A., & Fersht, A. R. (1992) *J. Mol. Biol. 224*, 733−740.

Ito, N., Phillips, S. E. V., Stevens, C., Ogel, Z. B., McPherson, M. J., Keen, J. N., Yadav, K. D. S., & Knowles, P. F. (1991) *Nature 350*, 87−90.
Jasanoff, A., & Weiss, M. A. (1993) *Biochemistry 32*, 1423−1432.
Klein, B., Zhang, X.-G., Lu, Z.-Y., & Bataille, R. (1995) *Blood 85*, 863−872.
Kochoyan, M., Keutmann, H. T., & Weiss, M. A. (1991) *Biochemistry 30*, 7063−7072.
Kossiakoff, A. A., Somers, W., Ultsch, M., Andow, K., Muller, Y. A., & deVos, A. M. (1994) *Protein Sci. 3*, 1697−1705.
Kunkel, T. A., Roberts, J. D., & Zakour, R. A. (1987) *Methods Enzymol 154*, 367−382.
Lakowicz, J. R. (1983) in *Principles of Fluorescence Spectroscopy*, Plenum Press, New York.
Loewenthal, R., Sancho, J., & Fersht, A. R. (1991) *Biochemistry 30*, 6775−6779.
Lovejoy, B., Cascio, D., & Eisenberg, D. (1993) *J. Mol. Biol. 234*, 640−653.
Macura, S., Huang, Y., Suter, D., & Ernst, R. R. (1981) *J. Magn. Reson. 43*, 259−281.
Manoleras, N., & Norton, R. S. (1992) *J. Biomol. NMR 2*, 485−494.
Marion, D., & Wüthrich, K. (1983) *Biochem. Biophys. Res. Commun. 113*, 967−974.
Matthews, J. M., Ward, L. D., Zhang, J. G., & Simpson, R. J. (1996) in *Techniques in Protein Chemistry* (Marshak, D. R., Ed.) Vol. 7, pp 449−457, Academic Press, New York.
Morton, C. J., Bai, H., Zhang, J.-G., Hammacher, A., Norton, R. S., Simpson, R. J., & Mabbutt, B. C. (1995) *Biochim. Biophys. Acta 1249*, 189−203.
Mosmann, T. (1983) *J. Immunol. Methods 65*, 55−63.
Muñoz, V., & Serrano, L. (1994) *Nat. Struct. Biol. 1*, 399−409.
Murakami, M., Hibi, M., Nakagawa, N., Nakagawa, T., Yasukawa, K., Yamanishi, K., Taga, T., & Kishimoto, T. (1993) *Science 260*, 1808−1810.
Narazaki, M., & Kishimoto, T. (1994) in *Guidebook to cytokines and their receptors* (Nicola, N. A., Ed.) pp 1−7, Oxford University Press, Oxford.
Nishimura, C., Watanabe, A., Gouda, H., Shimadada, I., & Arata, Y. (1996) *Biochemistry 35*, 273−281.
Paonessa, G., Graziani, R., De Serio, A., Savino, R., Ciapponi, L., Lahm, A., Salvati, A. L., Toniatti, C., & Ciliberto, G. (1995) *EMBO J. 14*, 1942−1951.
Proudfoot, A. E. I., Brown, S. C., Bernard, A. R., Bonnefoy, J.-Y., & Kawashima, E. H. (1993) *J. Protein Chem. 12*, 489−497.
Rucker, S. P., & Shaka, A. J. (1989) *Mol. Phys. 68*, 509−517.
Santoro, M. M., & Bolen, D. W. (1988) *Biochemistry 27*, 8063−8068.
Savino, R., Lahm, A., Salvati, A. L., Ciapponi, L., Sporeno, E., Altamura, S., Paonessa, G., Toniatti, C., & Ciliberto, G. (1994a) *EMBO J. 13*, 1357−1367.
Savino, R., Ciapponi, L., Lahm, A., Demartis, A., Cabibbo, A., Toniatti, C., Delmastro, P., Altamura, S., & Ciliberto, G. (1994b) *EMBO J. 13*, 5863−5870.
Simpson, R. J., Moritz, R. L., van Roost, E., & van Snick, J. (1988a) *Biochem. Biophys. Res. Commun. 157*, 364−372.
Simpson, R. J., Moritz, R. L., Rubira, M. R., & van Snick, J. (1988b) *Eur. J. Biochem. 176*, 187−197.
Simpson, R. J., Hammacher, A., Smith, D. K., Matthews, J. M., & Ward, L. D. (1997) *Protein Sci. 6*, 929−951.
Somers et al. (1997) *EMBO J. 16*, 989−997.
Sprang, S. R., & Bazan, J. F. (1993) *Curr. Opin. Struct. Biol. 3*, 815−827.
Ultsch, M., de Vos, A. M., & Kossiakoff, A. A. (1991) *J. Mol. Biol. 22*, 306−312.
van Snick, J., Cayphas, S., Vink, A., Uyttenhove, C., Coulie, P., Rubira, M. R., & Simpson, R. J. (1986) *Proc. Natl. Acad. Sci. U.S.A. 83*, 9679−9683.
Ward, L. D., Zhang, J.-G., Checkly, G., Preston, B., & Simpson, R. J. (1993a) *Protein. Sci. 2*, 1291−1300.
Ward, L. D., Hammacher, A., Zhang, J.-G., Weinstock, J., Yasukawa, K., Morton, C. J., Norton, R. S., & Simpson, R. J. (1993b) *Protein Sci. 2*, 1472−1481.
Ward, L. D., Howlett, G. J., Discolo, G., Yasukawa, K., Hammacher, A., Moritz, R. L., & Simpson, R. J. (1994) *J. Biol. Chem. 269*, 23286−23289.
Ward, L. D., Matthews, J. M., Zhang, J.-G., & Simpson, R. J. (1995) *Biochemistry 34*, 11652−11659.
Wells, J. A. (1996) *Proc. Natl. Acad. Sci. U.S.A. 93*, 1−6.
Wery, J. P., Schevitz, R. W., Clawson, D. K., Bobitt, J. L., Dow, E. R., Gamboa, J., Goodson, T., Hermann, R. B., Kramer, R. M., McClure, D. B., Mihelich, E. D., Putnam, J. E., Sharp, J. D., Strak, D. H., Teater, C., Warrick, M. W., & Jones, N. D. (1991) *Nature 352*, 79−82.
Xu, G.-Y., Hong, J., McDonagh, T., Stahl, M., Kay, L. E., Seehra, J., & Cumming, D. A. (1996) *J. Biomol. NMR 8*, 123−135.
Yamasaki, K., Taga, T., Hirata, Y., Yawata, H., Kawanishi, Y., Seed, B., Taniguchi, T., Hirano, T., & Kishimoto, T. (1988) *Science 241*, 825−828.
Zhang, J.-G., Moritz, R. L., Reid, G. E., Ward, L. D., & Simpson, R. J. (1992) *Eur. J. Biochem. 207*, 903−913.

BI962939W